Geodinamica Acta
Publication details, including instructions for authors and subscription information:
http://www.tandfonline.com/loi/tgda20

Different PT paths recorded in a tectonic mélange (Voltri Massif, NW Italy): implications for the exhumation of HP rocks

Laura Federico [a], Laura Crispini [a], Marco Scambelluri [a] & Giovanni Capponi [a]
[a] Dipartimento per lo Studio del Territorio e delle sue Risorse, University of Genova, C.so Europa 26, 16132, Genova, Italy
Published online: 13 Apr 2012.

Geodinamica Acta 20/1-2 (2007) 3-19

Geodinamica Acta

Different PT paths recorded in a tectonic mélange (Voltri Massif, NW Italy): implications for the exhumation of HP rocks

Laura Federico*, Laura Crispini, Marco Scambelluri, Giovanni Capponi

Dipartimento per lo Studio del Territorio e delle sue Risorse, University of Genova, C.so Europa 26, 16132 Genova (Italy)

Received: 30/11/05, accepted: 30/06/06

Abstract

The Cascine Parasi Mélange (CPM) of the high-pressure, meta-ophiolitic Voltri Massif (Ligurian Western Alps), consists of a foliated chlorite-actinolite greenschist matrix enclosing lenses of metabasites and metasediments. The surrounding units consist of serpentinites not enclosing these metamorphic rocks. The matrix records three sets of folds: (i) Dm1/Dm2 (blueschist to greenschist-facies conditions), which can be correlated to folds in the metasedimentary blocks; (ii) Dm3, which are the most obvious in the field and which partially re-orient the previous structures. The metabasite lenses preserve internal High-Pressure (HP) schistosities unrelated to the matrix foliation. The lenses equilibrated at different peak metamorphic conditions (ranging from eclogite- to blueschist-facies) and some recorded the prograde transition from lawsonite-bearing assemblages to garnet blueschists. Individual lenses display different segments of typical subduction PT paths which apparently converge in the blueschist facies. A late stage greenschist-facies re-equilibration is particularly widespread at the rims of the HP lenses. These structural and metamorphic features suggest that the mélange was active during early phases of the structural evolution of the area, at least through the exhumation and emplacement of the HP blocks into shallower crustal levels at conditions transitional from blueschist- to greenschist-facies; the older history is only preserved inside the blocks.

Keywords: tectonic mélange, high-pressure metamorphism, Ligurian Alps, exhumation

1. Introduction

According to Raymond [1], a mélange is 'a mappable body of rock characterized both by the lack of internal continuity of contacts or strata and by the inclusion of fragments and blocks of all sizes, exotic and native, embedded in a fragmented matrix of finer grained material'. Many different mechanisms, from purely sedimentary sliding to synmetamorphic ductile deformation can account for the genesis of mélanges. In a tectonic mélange, the lack of internal continuity and the fragmentation of the matrix must be related to some deformation mechanism.

In this paper we analyse a tectonic mélange (Cascine Parasi mélange - CPM) in the meta-ophiolitic Voltri Massif of the Ligurian Alps (Fig. 1). The mélange is made up of metre- to decametre-scale blocks and lenses of metabasites and metasediments embedded in a foliated chlorite-actinolite greenschist matrix. Strain partitioning between blocks and matrix is striking. The mélange zone is hosted by country serpentinites which do not enclose elsewhere such a variety of metamorphic rocks. As a consequence, the mixing of rocks not originally adjacent is evidence for large-scale transport achieved inside this high strain zone.

We performed a detailed fieldwork and structural analysis, in order to understand the tectonic setting of the area and the possible deformation mechanism responsible for mélange formation. Subsequent petrographic and petrologic studies

* Corresponding author.
Tel: +39 0103538292 - *Fax:* +39 010352169
E-mail address: federico@dipteris.unige.it

doi:10.3166/ga.20.3-19

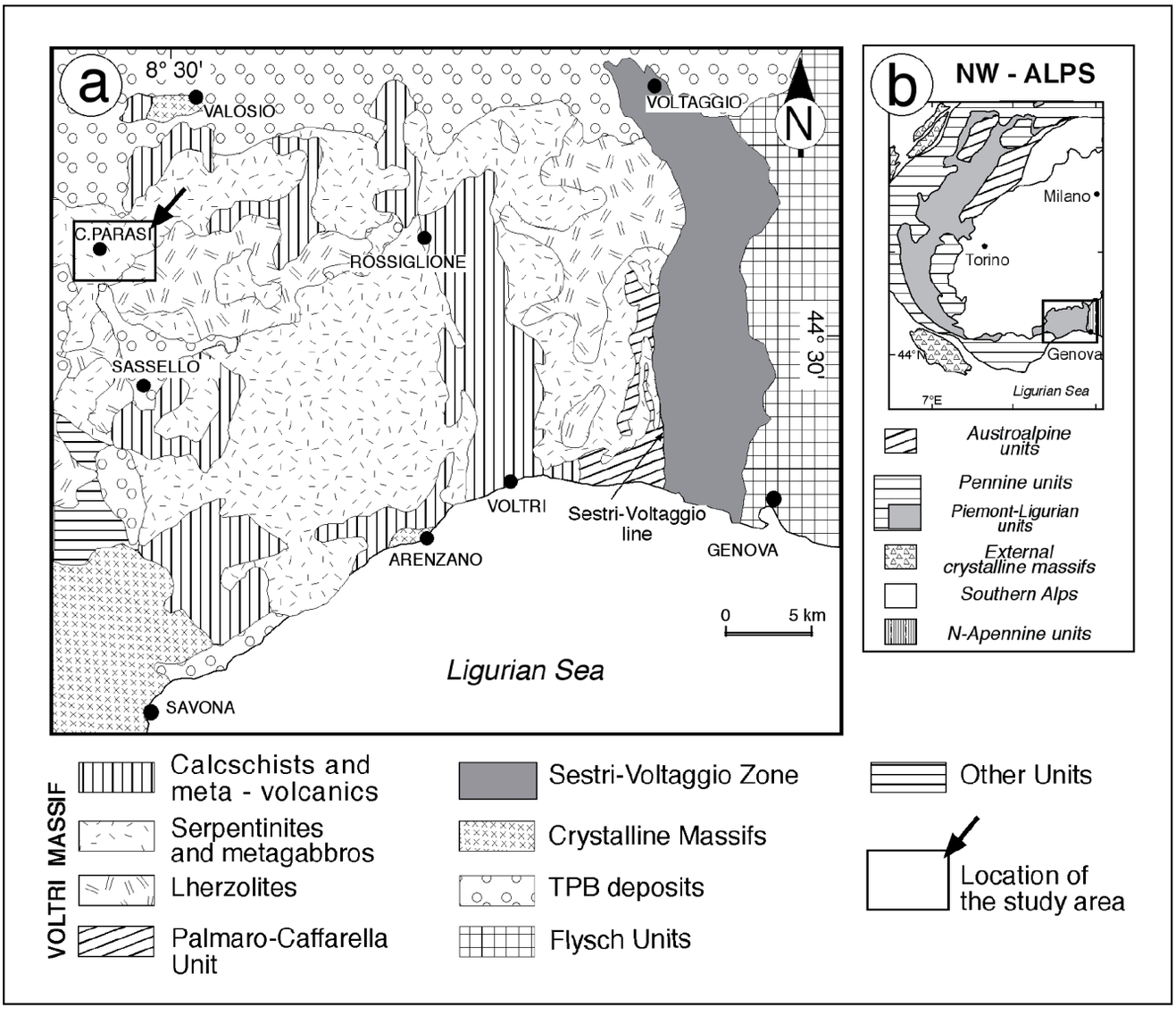

Fig. 1: Sketch map of the Voltri Massif (TPB = Tertiary Piemontese Basin) **(a)** with its location in the Western Alps **(b)**. Palmaro - Caffarella unit = meta-ophiolites and metasediments in blueschist facies.

enabled to trace the PT evolution of the different rock bodies and of the matrix.

A discussion follows on the possible role of this structure in the context of the exhumation of the High Pressure (HP)-rocks, also in light of recent tectonic models involving large transport of HP-rocks inside the 'subduction channel', formed at the interface between the subducting and the overriding plate because of hydration of the mantle wedge (e.g. [2,3]).

2. Geological background

The Voltri Massif (Ligurian Western Alps) is made up of meta-ophiolitic rocks associated with metasediments and subcontinental mantle slices (Fig. 1), which underwent a complex Alpine tectono-metamorphic history from high-pressure conditions to variable retrogressive overprints.

The Voltri Massif meta-ophiolitic rocks are serpentinites with metagabbros and metabasites; subcontinental mantle is represented by lherzolites with minor pyroxenite and dunite bodies. The metasediments cover the whole range from quartz-schists to calcschists to micaschists.

During Alpine subduction these rocks reached depths in the range of 50-75 km [4-7] under eclogite or blueschist facies; they underwent subsequent retrogression at decreasing pressure conditions up to final re-equilibration in greenschist facies. The Voltri eclogites display peak garnet + omphacite + rutile assemblage formed at T = 450-500 °C and pressures between 13 and 20 kbars [8, 4, 6]. The HP-LT (high pressure - low temperature) stages are best preserved in the mafic rocks, whereas the greenschist facies assemblages are widespread in metasediments [9]. The latter rocks display a relic assemblage of paragonite + phengite + oxydes ± garnet ± epidote ± rutile, related to the eclogite-facies stage [7]. This

MELANGE			COUNTRY ROCK (Cascine Parasi area)			VOLTRI MASSIF			
Deformation	Metamorphism	Fabric	Deformation	Metamorphism	Fabric	Deformation	Metamorphism	Fabric	Tectonic phase
Dmb	eclogite/ blueschist	Si	?	?	?	pre-D1	eclogite to blueschist	rootless hinges of isoclinal folds and related schistosity	subduction
Dm1/Dm2	blueschist to greenschist	Sm-1							
			D1/D2	greenschist	CF	D1/D2	Na-amp greenschist to greenschist s.s.	CF	exhumation and nappe emplacement
			EPF	greenschist	shear bands	EPF	greenschist	shear bands	
Dm3	(low greenschist) non metamorphic	Sm	D3	(low greenschist) non metamorphic	rough cleava-ge	D3	low greenschist	rough cleavage	collision
Dm3tr	non metamorphic	shear bands							
Dm4	non metamorphic	/	D4	non metamorphic	/	D4	zeolite facies/non metamorphic	/	post-collisional transtension

TIME

Table 1: relationships between studied deformation events in the mélange, its country rock (the serpentinites surrounding it) and Voltri Massif after Capponi and Crispini [9]. Dm = deformations inside the mélange.

paragenesis is usually retrogressed into lower Si^{4+} -phengite and chloritoid; the final re-equilibration in greenschist-facies conditions is testified to by the muscovite + chlorite + albite + biotite ± sphene ± oxydes association [7, 9, 10].

These rocks show several superposed deformations, achieved under different tectonic conditions and ranging from a ductile to a brittle regime. They can be summarized as follows (Table 1) [9]:

➢ HP-LT deformations (pre-D1) linked to subduction: eclogite facies foliation and rootless hinges of isoclinal folds; these structures occur all over the massif, but show no continuity and are not easily correlated.

➢ Na-amphibole greenschist to greenschist facies s.s. deformations (D1 and D2): D1 and D2 folds and related schistosity are widespread at the scale of the entire massif. The D1 and D2 schistosity, plus the previous foliation (including the lithological surface), produce the Composite Fabric (CF), which is the most evident surface in the field and controls the contacts between different lithologies.

➢ Ductile structures recording extension parallel to the foliation (hereafter EPF): they range from shear bands, boudins, foliation boudinage and extensional veins [11] and occur under greenschist facies conditions. These structures record an extension acting sub-parallel to the main planar anisotropy: they do not automatically imply regional extension [12], but only in the case that the schistosity is close to the horizontal before deformation. These structures and D1/D2 folds are linked to the exhumation and nappe emplacement events.

➢ D3 and D4 folds: open and chevron folds with no pervasive metamorphic recrystallization. Reverse shear zones, D3 and D4 structures developed in a collisional and post-collisional tectonic regime.

During collisional events, the original contacts between ultramafites and metasediments were often reactivated by ductile to semi-brittle deformations, which at least in one case led to the formation of a mélange zone, described by Vissers *et al*. [13]. Differently from the tectonic mélange presented here, the mélange described by Vissers *et al*. [13] contains blocks belonging only to the two surrounding lithologies and clearly formed during late-stage greenschist-facies thrust tectonics.

The Voltri Massif and the Ligurian Alps are unconformably overlain by late- to post-orogenic deposits belonging to the Tertiary Piemontese Basin. These sediments are locally folded and tilted by D4 structures.

3. Structural setting

The studied area is characterized by wide outcrops of serpentinite and minor lherzolite and by small outcrops of Tertiary conglomerates. The Cascine Parasi mélange zone is bounded by tectonic contacts and occurs inside pervasively foliated serpentinite. The mélange outcrops in two distinct areas ca. 800 m apart: here we will focus on the southernmost one (ca. 300 m long and 80 m wide), which is the best exposed.

The main schistosity of the country serpentinite is a composite foliation (CF) developed during the superposition of the synmetamorphic D1/D2 deformation events (see previous paragraph).

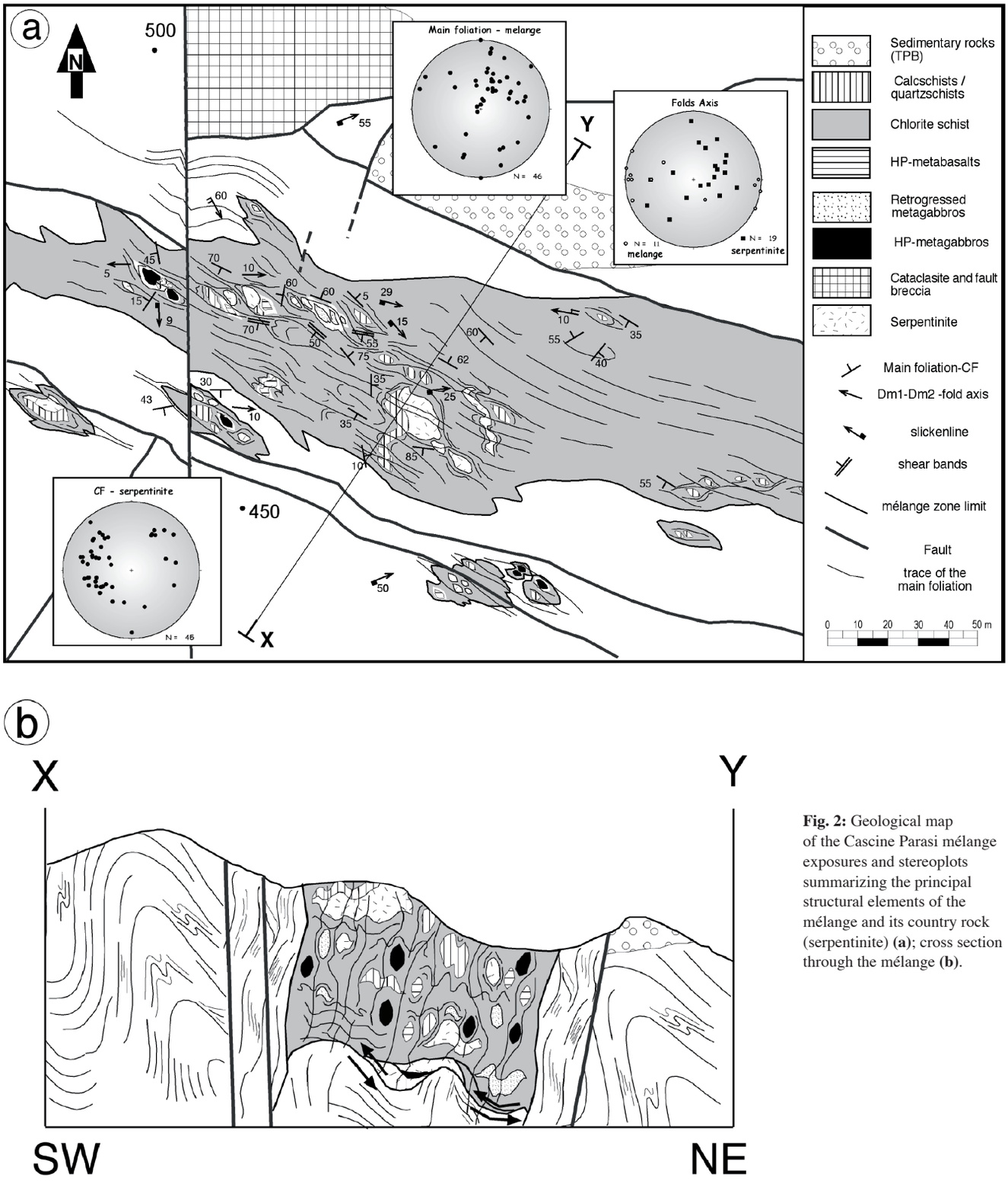

Fig. 2: Geological map of the Cascine Parasi mélange exposures and stereoplots summarizing the principal structural elements of the mélange and its country rock (serpentinite) **(a)**; cross section through the mélange **(b)**.

The CPM is made up of m-scale lenses (MBs) (Fig. 2a and b, Fig. 3a) of metagabbro, metabasite, metasediments and serpentinite, enclosed in a schistose chlorite-rich matrix, which grades into the host serpentinites. In the mélange, structures are heterogeneously distributed due to the effect of strain partitioning between the competent MBs and the soft matrix. Strain concentration in the chlorite-rich matrix is very striking in the field. The strong contrast between the MBs and the matrix causes the blocks to weather out from the matrix as boulders (Fig. 3a).

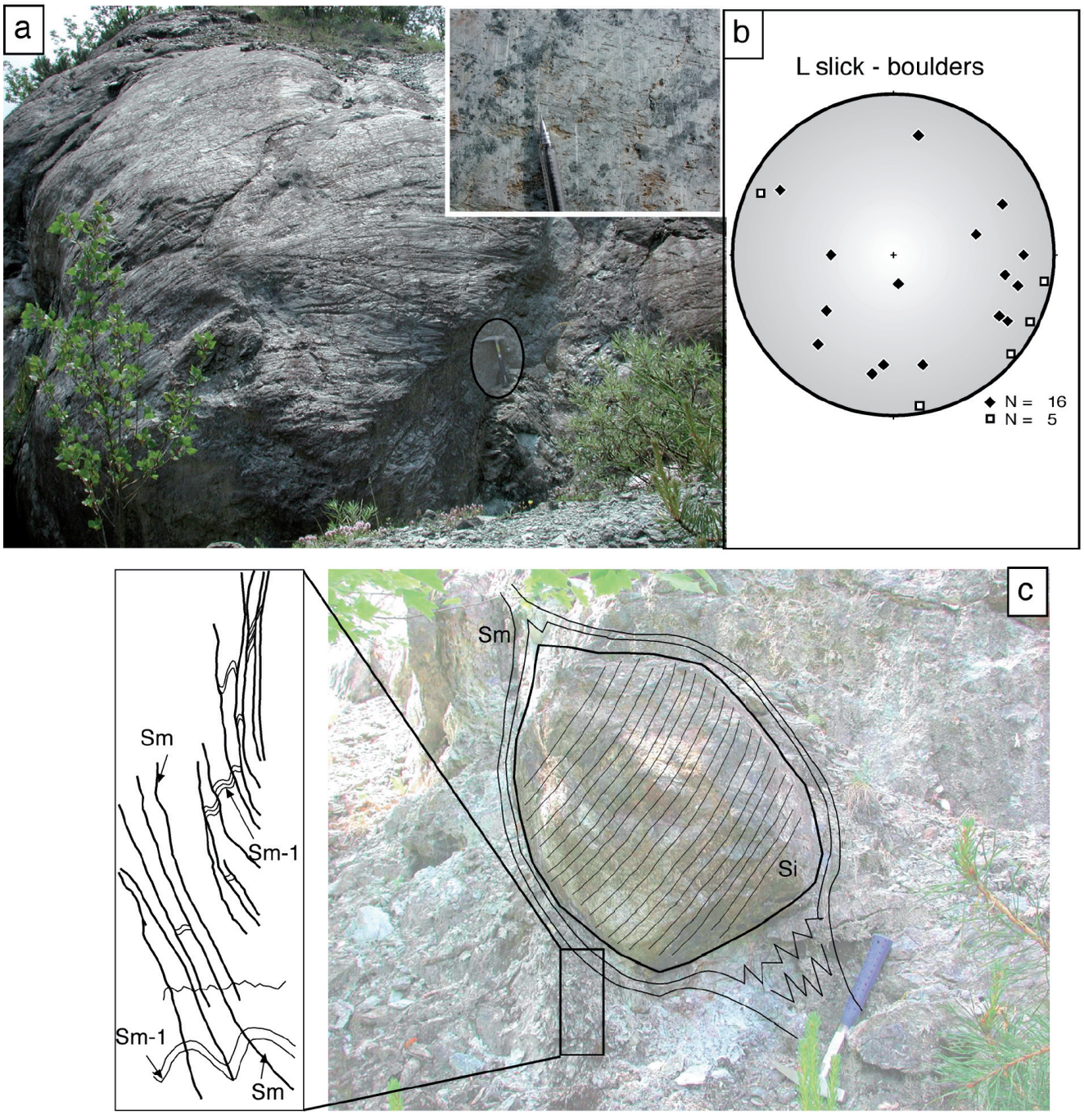

Fig. 3: Slickenlines on the polished surfaces of the boulders **(a)** and orientation of the two sets **(b)**: one NE-SW steeply to moderately plunging and the other WNW-ESE shallowly plunging. **(c)** Relationships between the internal schistosity of the boulders (Si) and the foliations of the mélange matrix (see text for details).

3.1. The mélange

In the matrix at least three superposed sets of folds can be recognized: Dm1, Dm2, Dm3 (the acronym "Dm" refers to deformations observed inside the mélange). Dm1 and Dm2 synmetamorphic folds are non-cylindrical, S-SW vergent (Fig. 2b); the fold axes have a main E-W trend with low plunge (Fig. 2a). These structures can be associated to a sub-horizontal shortening phase. Such folds display a pervasive mylonitic axial plane foliation which strikes WNW-ESE, dips towards ENE and is partly reoriented by later Dm3 folds. At the microscale the schistosity is characterized by a greenschist facies assemblage of chlorite + actinolite + apatite + sphene + ores ± epidote ± rutile with rare relics of blue amphibole (see par. 4.4). The presence of Na-amphibole relics suggests that the matrix accomplished deformation since HP-LT conditions and was pervasively re-equilibrated

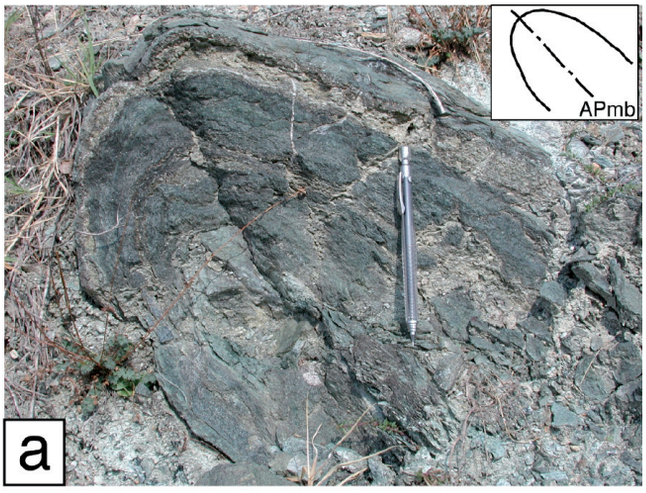

Fig. 4: Photographs of the oldest set of folds in the metasedimentary boulders **(a)**, APmb = trace of the axial plane of folds inside the blocks (deformation phase Dmb in Table 1). Note Na-amphibole lineations (Lmin) parallel to the fold axis **(b). (c)** Dm3 folds in mélange matrix (APm3 = trace of the axial plane of Dm3 folds).

in the greenschist facies.

Dm3 folds are irregular and non-cylindrical (Fig. 4c). They display an axial plane-foliation with NNW-SSE strike, steeply dipping to the W (Fig. 2b), with plunging axes scattered around NNW-SSE trends. They deform Dm1-Dm2 folds and in places the Dm3 foliation transposes all the previous structures, producing the most evident foliation in the field (Sm) (Fig. 3c).

MBs of metagabbros and metabasalts have internal metamorphic foliations (Si) witnessing deformations older than Sm (Fig. 3c); these deformations are comprehensively indicated as Dmb in Table 1. These foliations developed at variable HP conditions and cannot be correlated neither from one block to the other nor with the matrix.

At least two synmetamorphic sets of folds have been recognized in the metasedimentary lenses. The older set is represented by disrupted, non-cylindrical intrafolial folds, with axial plane-related foliation and mineral stretching lineations characterized by the stability of Na-amphiboles (Fig. 4a, b). The Na-amphibole lineations are nearly parallel to the fold axis. The younger set consists of open folds with E-W trending axes coeval with recrystallization in greenschist facies. This phase is clearly correlatable with Dm2 folds of the matrix.

The Dm1/Dm2 deformation events are related to a top-to-S-SW phase of thrusting recognized throughout the whole area that developed under Na-amphibole greenschist to greenschist s.s. conditions. Due to later folding, the original shear zone kynematics cannot be reconstructed. However, the present-day geometry suggests a reverse sense of shear. In view of their vergence and tectonic style the Dm1/Dm2 can be linked to the nappe emplacement deformation phase, which in the Ligurian Alps is typically top-to-S-SW vergent (e.g. [14,15]).

The Dm3 deformation is consistent with a phase of sinistral transpression accomodated along WNW-ESE striking shear zones reactivated by later faults at the margins of the mélange (Fig. 2a).

After Dm3 a phase of vertical shortening (Dm3tr in Table 1) generates E-W striking discrete shear bands that in places deflect Sm (Fig. 2a) and are associated to stretching lineations with a transtensional component.

Deeply carved slickenlines and grooves occur on the polished surfaces of metabasite and serpentinite MBs (Fig. 3a). Two sets of lineations are consistently observed throughout the whole mélange zone; one set is steeply to moderately plunging NE-SW and the other set is shallowly plunging WNW-ESE (Fig. 3b). These lineations originated during the progressive deformation from Dm1/Dm2 to Dm3. Slickenlines have been produced by the shearing between the more competent MBs and the surrounding matrix due to strain partitioning during folding event.

3.2. The country rock

In the country serpentinite structures linked to the regional deformation events have different features and styles relative

SAMPLE	PROTOLITH	PROGRADE RELICS	PEAK ASSEMBLAGE	RETROGRESSION
Eclogite/blueschist metagabbros				
C24	Gabbro		Na-cpx+lws+tr±Na-amp	minor chl, ab, bt
C30	Gabbro	Na-cpx1, lws (?)	Na-cpx2+ +czo1+spn+ph±pg	czo2, ab, chl
C1	Gabbro	Na-cpx1, rt	Na-cpx2+ +spn+chl+ep±Na-amp	minor Ca-amp, ab, cal, ms, chl
CP8	Gabbro		Na-cpx+ep+ph	-
Eclogite/blueschist metabasites				
C27	Mafic rock	Na-amp	Grt+Na-cpx+ +spn+chl+ph	chl, ab, ep, ms
CP5	Basalt	Na-cpx, grt, Fe-Na-amp1	Na-amp2+ph+ep+spn	Na-Ca amp, ms, ab, chl
CP2	Basalt	grt, Na-amp, rt	Na-amp2+ep+ph	chl, ab
VR81	Mafic sediment (?)	Na-amp1, grt, rt	Na-amp2+ph+Fe-ep+ +spn	Na-Ca amp, chl
C9	Basalt	spn, ph, lws (?), Na-amp	Na-amp1+grt+ph1+spn	Na-amp2, ph2, ep, spn
Eclogite/blueschist metasediments				
C8	Sediment		Na-amp +grt+ ph+ep±spn±ap± ores	Ca-amp, ab
C13	Sediment	Na-cpx, grt	Na-amp+ph+ep+qtz	cal, bt, ph
CP3	Sediment	Na-amp, lws (?)	Na-amp+ph+ +chl+ep+qtz+ cal±grt	chl, ab
C46	Sediment	mag, Mg-amp, rt	Na-amp+grt+Na-cpx+ +ph+qtz+ap	Na-Ca amp, bt

Table 2: summary of mineral associations in the studied samples. Abbreviations are after Kretz [16]. See Appendix 1 for much detail on the mineral compositions.

to the enclosed mélange zone.

The older folds (D1/D2, Table 1) are almost completely transposed. The main foliation developed mostly during D1/D2 and is deformed by at least two superposed deformations, characterized by:

1) synmetamorphic shear bands (EPF, Table 1) generated during a top-to-E extensional phase. They are accompanied by a serpentine + magnetite ± calcite ± talc ± chlorite association testifying greenschist facies conditions. Comparable overprinting relationships between EPF and D1/D2 folds have been recognized elsewhere in the Voltri Massif (Table 1). Here such an overprint has been attributed to the latest stage of a continuous progressive deformation which starts in the Na-amphibole greenschist-facies and ends in the greenschist facies field [9].

2) metre-scale folds with open and chevron geometry, not accompanied by recrystallization. Axial planes are N-S striking and steeply dipping to the E (Fig. 2a and b). These folds can be correlated to the Dm3 deformation in the mélange zone (Table 1)

Later brittle deformation finally produces ESE-WNW striking normal and oblique slip faults which dissect also the mélange area (D4 and Dm4, Fig. 2).

The structural and metamorphic features described above suggest that the mélange was active during early stages of the structural evolution of the area, at least through the exhumation and emplacement of the nappe system. In the chlorite matrix rare blue amphibole relics testify for coupling between blocks and matrix already at HP conditions. The oldest deformation yet recorded by the mélange is thus the synmetamorphic shearing enhancing blueschist re-crystallization. Fragments of the older history are only preserved inside the MBs.

4. Petrography of the mélange blocks

The mélange blocks consist of different lithologies: metasediments (quartz schist and calc-schist), metagabbro, metabasalt and serpentinite. Striking features are: (i) the exotic nature of some lenses (mafic rocks and metasediments) which are absent in the country rocks over kilometric distances and in some case (see paragraph 6) have no analogues at all in the Voltri Massif; (ii) the different peak PT conditions recorded by the various MBs.

Among the samples studied, we selected the ones which best preserve the HP-assemblages and which show contrasting PT paths (Table 2). A detailed description of each sample is given in Appendix 1. Samples have been grouped according to similar protoliths and metamorphic history.

4.1. Eclogite/blueschist metagabbros

These samples range from strongly deformed to undeformed metagabbro, with HP Na-clinopyroxene + lawsonite or Na-clinopyroxene + epidote assemblages subsequently partialy retrogressed to greenschist facies compatibilities (Table 2). They usually display different generations of pyroxene, with magmatic augite overgrown by omphacite along the rims and cleavage planes; the jadeite content is usually increasing in the younger-generation pyroxenes (Fig. 5a and c and Table 3).

4.2. Eclogite/blueschist metabasites

These samples are characterized by a pervasive schistosity which developed under peak (i) eclogite- (C27, CP5) or under (ii) garnet- to epidote-blueschist facies (CP2, VR81 and C9). Eclogites preserve their peak garnet + Na-clinopyroxene assemblage (C27), which is subsequently overprinted by variable degrees of blueschist-facies recrystallization (CP5). The blueschist-facies rocks show a typical peak Na-amphibole + garnet + phengite assemblage; garnet is then overgrown by epidote. Sample C9

	C24 P1A1 Cpx1 c	C24 P1A2 Cpx1 r	C24 S1A4 Cpx2	C27 S1A5 Cpx	C27 S2A1 Grt c	C27 S2A4 Grt r	CP5 S3A1 Grt c	CP5 S3A3 Grt r	CP5 S3A6 Ph	CP5 S2A1 Na-amp2	C46 S1A7 Grt	C46 S2A5 Ph
SiO2	52.31	55.25	55.16	54.89	37.39	37.21	37.20	37.41	52.09	55.19	37.45	57.05
TiO2	0.51	0.04	0.13	0.12	0.21	0.13	0.25	0.08	0.25	0.1	0.24	0.09
Al2O3	4.38	7.38	7.30	8.10	20.24	20.63	19.87	20.29	22.92	10.46	20.11	17.88
Cr2O3	0.68	1.74	0.24	0.24	0.16	0.19	0.26	0.18	0.11	0.19	0.06	0.08
FeO	3.60	4.66	7.67	14.58	13.61	29.17	20.24	27.37	5.67	17.9	16.83	3.7
MgO	14.98	9.14	9.06	4.02	0.38	0.42	0.20	0.11	3.50	6.1	0.37	6.18
MnO	0,15	0.11	0.28	0.21	18.43	3.67	13.54	7.40	0.17	0.28	17.58	0.07
NiO	0.00	0.00	0.20	0.23	0.10	0.06	0.30	0.17	0.00	0.12	0.00	0.00
CaO	21.92	14.25	13.13	7.28	9.47	8.36	8.43	7.12	0.14	0.99	8.04	0.12
Na2O	1.41	6.69	7.34	10.28	0.00	0.00	0.00	0.00	0.00	6.63	0.00	0.20
K20	0.00	0,00	0,00	0,00	0.00	0.15	0.00	0..00	11.25	0.08	0.00	11.27
sum	99.94	99.26	100.51	99.95	99.99	99.84	100.29	100.13	96.10	98.04	100.68	96.64
Si	1.90	1.99	1.96	1.98	3.01	3.01	3.01	3.03	3.51	7.81	3.02	3.79
Ti	0.01	0.00	0.00	0.00	0.01	0.01	0.02	0.00	0.01	0.01	0.01	0.00
Al	0.19	0.31	0.31	0.34	1.92	1.97	1.90	1.94	1.82	1.74	1.91	1.40
Cr	0.02	0.05	0.01	0.01	0.01	0.01	0.02	0.01	0.01	0.02	0.00	0.00
Fe3+	0.06	0.13	0.23	0.41	-	-	-	-	0.10	0,39	-	0.00
Fe2+	0.05	0.01	0.00	0.04	0.92	1.97	1.37	1.85	0.22	1,73	1.13	0.21
Mg	0.81	0.49	0.48	0.22	0.05	0.05	0.02	0.01	0.35	1,25	0.04	0.61
Mn	0.01	0.00	0.01	0.01	1.26	0.25	0.93	0.51	0.01	0.03	1.20	0.00
Ni	0.00	0.00	0.01	0.01	0.01	0.00	0.02	0.01	0.00	0.01	0.00	0.00
Ca	0.86	0.55	0.50	0.28	0.82	0.72	0.73	0.62	0.02	0.15	0.69	0.01
Na	0.10	0.47	0.51	0.72	0.00	0.00	0.00	0.00	0.00	1.82	0.00	0.02
K	0.00	0.00	0.00	0,00	0.00	0.00	0.00	0.02	0.97	0.01	0.00	0.95
sum	4.00	4.00	4.00	4.00	8.01	8.00	8.02	7.99	7.02	14.97	8.00	6.99

Table 3: selected mineral analyses. C = core, R = rim

preserves relics of a prograde stage in lawsonite-blueschist facies as aggregates of phengite + chlorite + biotite ± paragonite, interpreted as pseudomorphs after lawsonite (Fig. 5e).

4.3. Eclogite/blueschist metasediments

The metasediments outcropping in the CPM can be classified as quartz schists and qtz-calcschists according to the proportion of quartz, carbonates and micas. All samples are strongly foliated and are characterized either by blueschist (C8, C13, CP3) or eclogite-facies (C46) assemblages (Table 2), followed by a more or less pervasive re-equilibration in the greenschist facies. In the blueschist sample C13, relics of Na-clinopyroxene and garnet suggest a previous, eclogitic stage. Aggregates of epidote + paragonite + quartz + phengite (Fig. 5g) can be interpreted as pseudomorphs after lawsonite, pointing to a prograde lawsonite-blueschist stage in sample CP3.

4.4. Mélange matrix

The matrix which envelopes the tectonic blocks is a chlorite-actinolite mylonitic schist. It appears to have been generated by the intense shearing deformation of the blocks and their metasomatic interplay with the enclosing serpentinites. At the microscale this rock is characterized by two superimposed foliations: an S_x with stable association of Mg-chlorite (up to 70-75% of the samples) + actinolite + sphene + ores (mainly magnetite), and an S_{x+1} defined by dark seams due to accumulations of insoluble material along dissolution surfaces and rare chlorite + actinolite grains. Aligned along S_x very rare glaucophane grains are partially replaced by actinolite (Fig. 6). The S_{x+1} is a crenulation cleavage, best developed in the chlorite-rich layers, which passes laterally into domains where S_x has been almost completely transposed and only some teared hinges are still preserved; in the amphibole-richer layers, on the contrary, S_{x+1} coincides with the axial plane of well preserved folds. At the microscale, the dominant foliation is usually a strongly attenuated and transposed crenulation cleavage. Relics of the original paragenesis (crystals of garnet, Na-clinopyroxene, rutile) are locally preserved on the rims of the eclogitic and blueschist blocks, where they become largely partially replaced by chlorite.

Fig. 5: Photographs of microstructures in the mélange blocks, plane-polarized light if not otherwise indicated. **(a)**, **(b)** sample C24; **(c)** sample C30; **(d)** sample C27; **(e)** pseudomorph after lawsonite in sample C9; **(f)** sample C8; **(g)** pseudomorph after lawsonite in sample CP3, cross-polarized light; **(h)** sample C46.

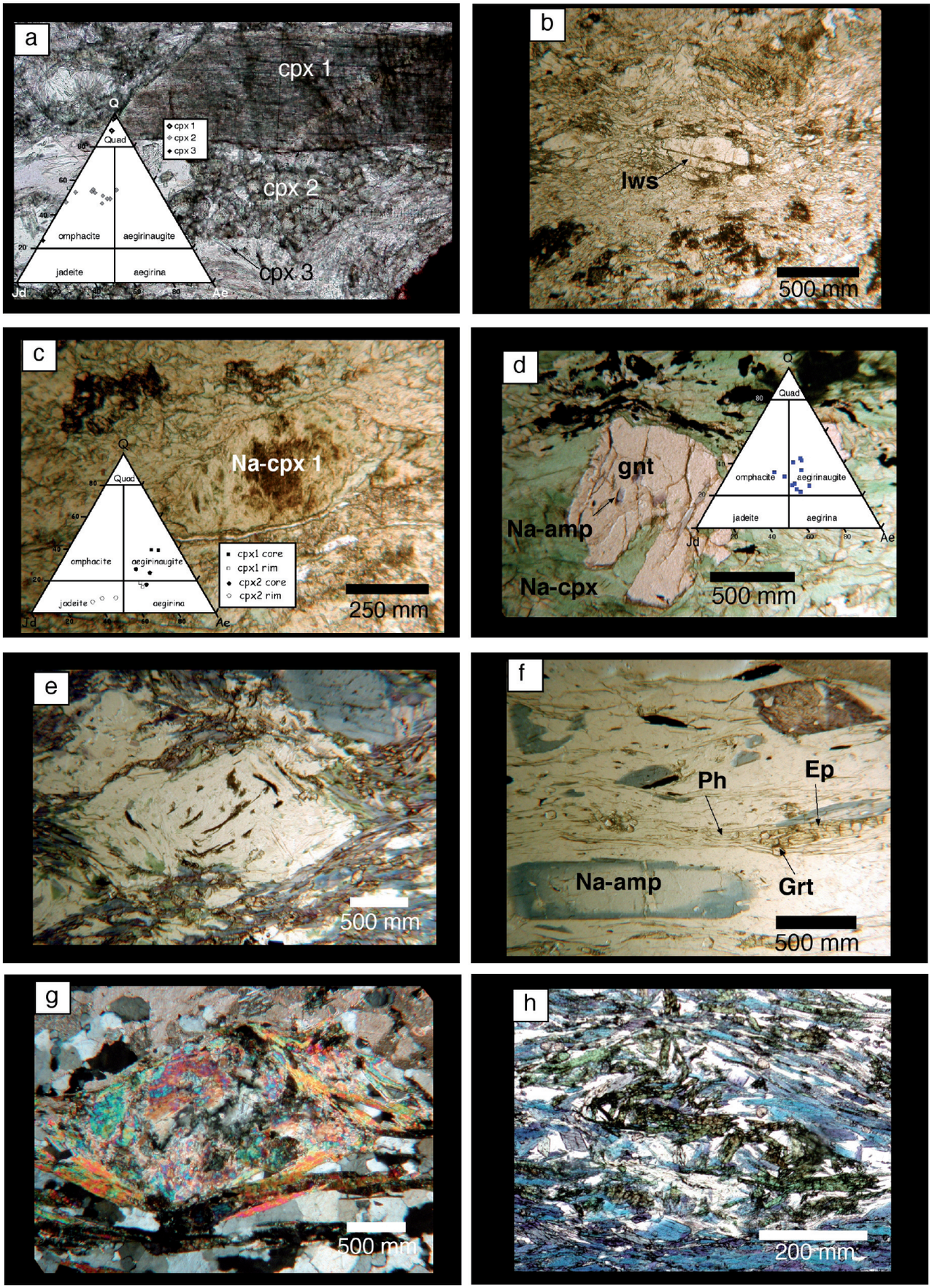

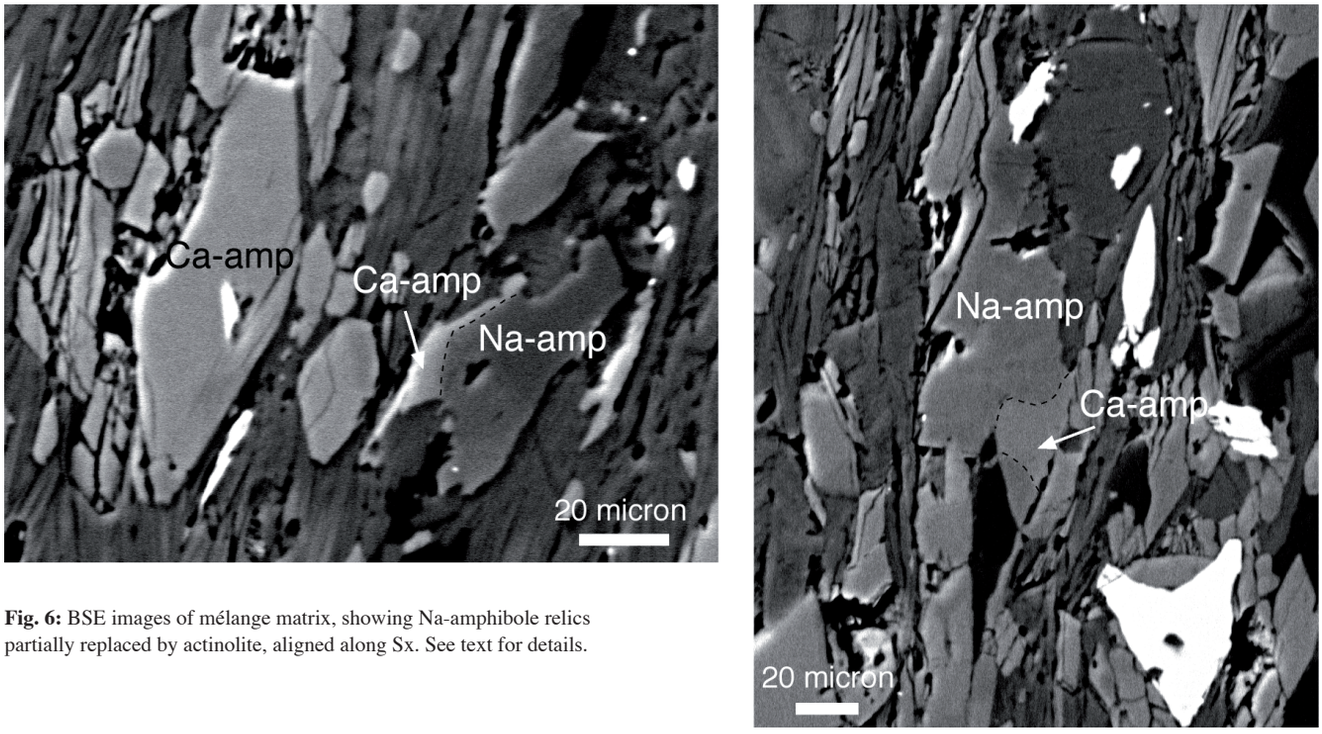

Fig. 6: BSE images of mélange matrix, showing Na-amphibole relics partially replaced by actinolite, aligned along Sx. See text for details.

The S_{x+1} in thin sections is the dominant foliation Sm in the mélange (Fig. 3), which is linked to the Dm3 phase (Table 1). The S_x schistosity was likely formed during the Dm1/Dm2 deformation events and can be correlated to the Sm-1.

The mineral assemblage of the matrix reveals a metasomatic reaction between the surrounding serpentinite and the minerals inside the boudins, resulting in an exchange of Ca, Fe and Al from the boudins to the serpentinite against Mg from the serpentinite (blackwall reactions, [17]). A similar situation has been described for the Syros mélange by Purcell [18]. The rare presence of Na-amphibole inside the matrix points to a metasomatic reaction in blueschist facies conditions. Subsequently, Na-amphibole has been pervasively replaced during greenschist-facies retrogression; this process has probably been enhanced by strain concentration in the matrix relative to the more competent blocks.

5. Pressure - temperature - deformation evolution

The mélange blocks record a range of evolutionary histories: some of them followed a prograde path from lawsonite-blueschist to garnet-blueschist facies (characterized by a Na-amphibole + garnet + phengite assemblage) (C9 metabasalt, CP3 metasediment); others are characterized by peak eclogite facies conditions (e.g. CP5) whereas some other display peak garnet-blueschist assemblages (e.g. VR81 - C13 - C8 - CP2). All these assemblages are overprinted by epidote-blueschist and greenschist facies retrograde assemblages.

Fig. 7a portrays the PT grid referred to a hydrated basaltic system together with the PT paths of the various mafic blocks. The breakdown reactions of lawsonite (numbers 1, 2 and 3) derive from the experimental work of Poli and Schmidt [19]. These reactions either involve Na-amphibole (low P) or garnet (high P) to produce zoisite. The stability fields of the assemblages garnet + glaucophane + mica (shaded area) and garnet + epidote + mica (striped horizontal area) are constrained by reactions calculated with the program VERTEX [21] in the NCFMASH system. K_2O and TiO_2 are neglected because they are chiefly present either in phengite or in rutile/sphene which are not involved in the most important reactions observed in our samples. Since most of the studied samples are iron-rich, Fig. 7a reports the reactions for the pure Fe-system, considering almandine and Fe-glaucophane end members. The only Mg-rich sample is metagabbro C24, characterized by the stable lawsonite + omphacite assemblage. Therefore, the lawsonite-out reactions 5 (lawsonite + omphacite = zoisite

Fig. 7: (a) PT diagram showing the different equilibration conditions recorded by the tectonic blocks of metabasites. Reactions: 1) lws + gl =pa + zo + chl + qtz, 2) lws + gl = pa + zo + py + qtz, 3) lws + gnt1 = zo + gnt2 + coe, experimentally determined by Poli & Schmidt [19]; 4) czo + gl + qtz + H_2O = tr + chl + ab, from Maruyama *et al*. [20]. The other reactions shown have been calculated with the program VERTEX [21] for the NCFMASH system and refer to the Fe-end members, except for reactions 5) lws + omph = zo+ pa + gl + qtz and 6) lws + jd = zo + pa + qtz which refer to the Mg-end members. Shaded area refers to the garnet-blueschist facies. **(b)** PT paths of studied metasediments in a petrogenetic grid for the system NFMASH (redrawn and modified after Guillot *et al*. [23]). Si isopleths of phengite from Massonne & Schreyer [24]; glaucophane stability field from Maresch [25]. Dashed ellipse represents PT estimates obtained using the THERMOCALC program (v.3.21, average PT calculation mode) for sample C46.
(c) summary of distinct PT paths recorded by the different tectonic blocks.

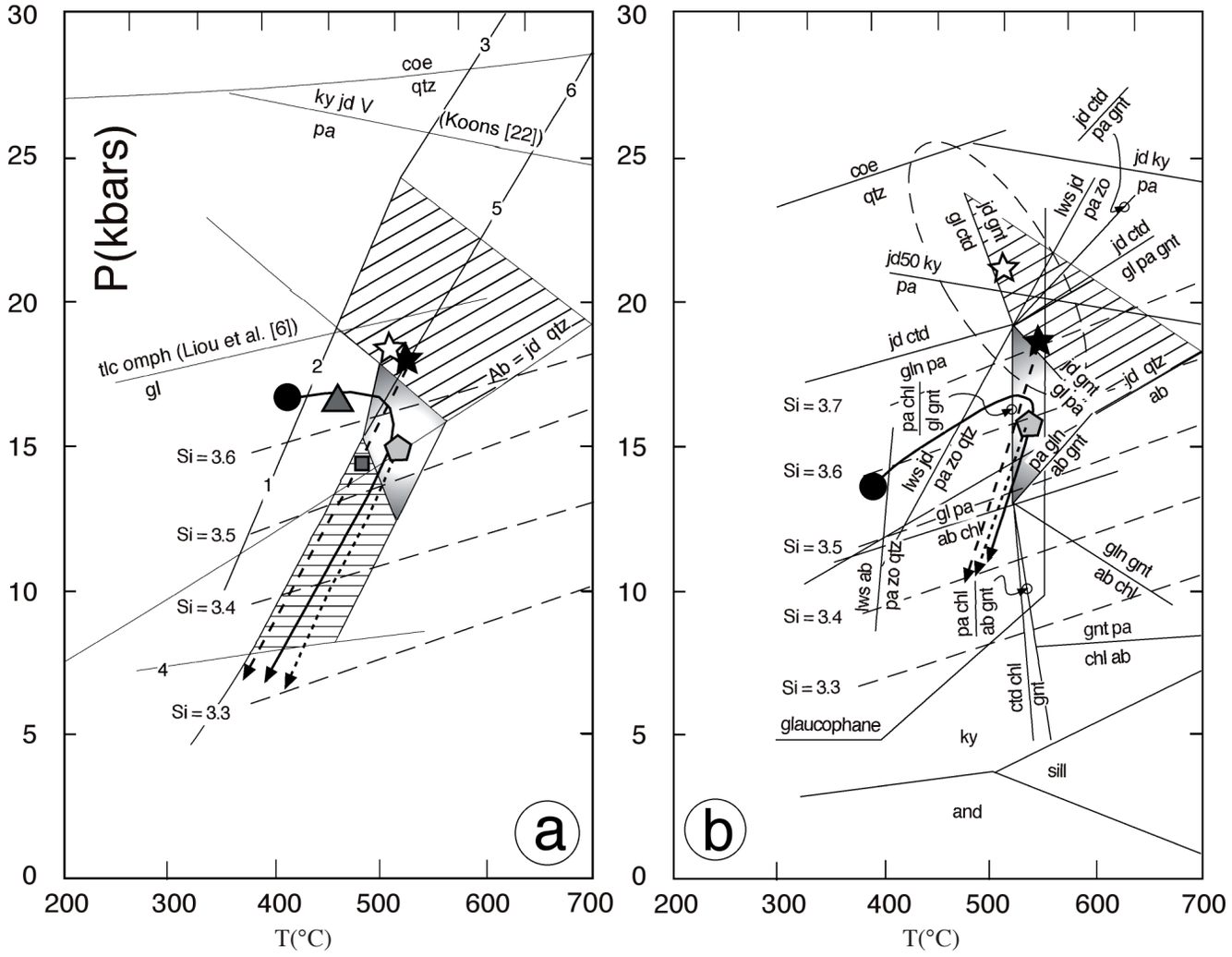

Caption fig. A

- **LWS + OMPH PEAK** (C24)
- **ECLOGITE PEAK** (C27)
- **ECLOGITE PEAK + RETROGRESSION** (CP5)
- **GNT-BLUESCHIST PEAK + LWS RELICS + RETROGRESSION** (C9)
- **GNT-BLUESCHIST PEAK + RETROGRESSION** (VR81 - CP2)
- **EP + OMPH PEAK** (C30, C1, CP8)

Caption fig. B

- **ECLOGITE PEAK** (C46)
- **ECLOGITE PEAK + RETROGRESSION** (C13)
- **GNT-BLUESCHIST PEAK + RETROGRESSION** (C8)
- **GNT-BLUESCHIST PEAK + LWS RELICS + RETROGRESSION** (CP3)

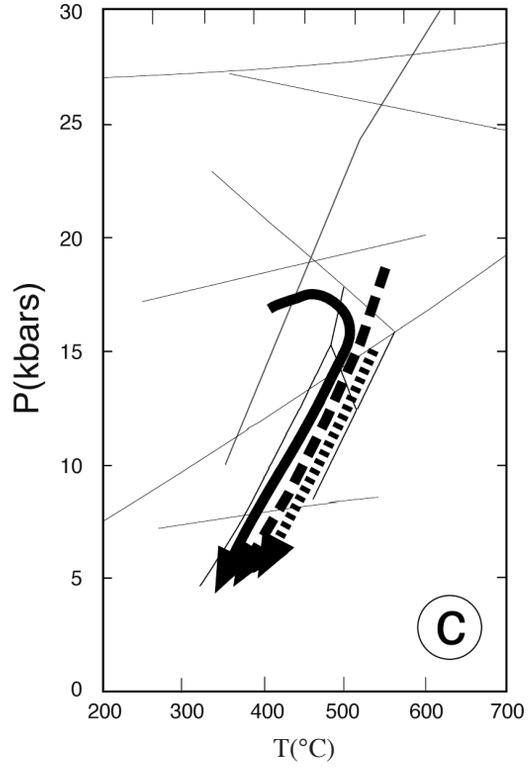

+ paragonite + glaucophane + quartz) and 6 (lawsonite + jadeite = zoisite + paragonite + quartz) have been computed for the Mg-end members.

The different symbols in Fig. 7a refer to samples or groups of samples which either record different peak metamorphic equilibration (without retrogression) or different successive steps of a coherent PT evolution. In particular the symbols refer to:

a) metagabbro with the syntectonic assemblage lawsonite + omphacite without retrogression (C24, filled triangle);

b) eclogite with typical synkinematic assemblage garnet + Na-clinopyroxene + sphene and minor retrogression to greenschist facies (C27, open star);

c) metabasalt showing a first equilibration stage in the eclogite facies, followed by retrogression and deformation through the garnet-blueschist and subsequently to the epidote-blueschist facies (CP5, filled star);

d) metabasalt which records the transition from lawsonite-blueschist to garnet-blueschist facies through prograde breakdown of lawsonite (reaction number 2 in Fig. 7a: lawsonite + Fe-glaucophane = zoisite + paragonite + garnet + quartz) (C9, filled circle). The garnet-blueschist assemblage underwent subsequent retrogression to the epidote-blueschist facies according to the reaction paragonite + almandine + quartz + omphacite = zoisite + glaucophane. This sample is affected by pervasive deformation at the garnet/epidote-blueschist transition;

e) metabasites with peak assemblage in the garnet-blueschist facies, dynamically retrogressed to the epidote-blueschist facies (VR81 and CP2, filled pentagon);

f) metagabbros characterized by the association of Na-clinopyroxene and clinozoisite ± Na-amphibole, with minor retrogression (C30, C1, CP8, filled square).

Fig. 7b shows the PT trajectories inferred for the metasedimentary blocks. The PT grid is built considering a NFMASH system with excess SiO_2 and H_2O, originally proposed by Guiraud *et al*. [26] and modified by Guillot *et al*., [23] for Fe-rich metapelites. This diagram does not consider phengite, but we can neglect it since it is stable throughout the metamorphic evolution and is not involved in the most important reactions observed in our samples. Moreover, Guiraud *et al*. [26] demonstrated that addition of K_2O does not produce significant shifts of the calculated reaction curves. A PT grid in the NFMASH system is considered suitable for discussing metapelite evolution in the high- and ultrahigh-pressure range also by Proyer [27]. The different symbols refer to samples showing a peculiar PT history, and in particular to:

a) a quartz schist with alternating layers of glaucophane + garnet + phengite and Na-clinopyroxene + garnet + phengite (Fig. 5h) pointing to equilibration in the eclogite facies (C46, open star). PT estimates obtained using the THERMOCALC program (v.3.21, average PT calculation mode) point to conditions of T = 506 ± 67 °C and P = 21.2 ± 3.6 kbars (uncertainties at the 2σ level). These estimates, though rather imprecise, are consistent with equilibration in the eclogite facies.

b) a quartz schist characterized by a blueschist-facies synkinematic assemblage of Na-amphibole + phengite + epidote + quartz. Rare Na-pyroxene grains and fine-grained garnet inclusions in both pyroxene and Na-amphibole suggest this sample previously equilibrated on the high-P side of the reaction jadeite + garnet = glaucophane + paragonite and was later retrogressed to blueschist facies compatibilities (C13, filled star). Minimum pressures of ca. 15 kbar (at 550°C) result from Si content of 3.55 - 3.65 p.f.u. in phengites.

c) a quartz schist characterized by the peak assemblage Na-amphibole + garnet, developed on the high-T side of the reaction paragonite + chlorite = glaucophane + garnet and on the low-T side of the reaction glaucophane + paragonite = jadeite + garnet, which represents the garnet-blueschist facies / eclogite facies limit (C8, filled pentagon). Garnet-phengite geothermometry [28] yields temperatures of 525 - 550 °C in the pressure range 12 - 17 Kb, in good agreement with the stability of garnet and Na-amphibole. Late chlorite and albite derive from destabilization of glaucophane through the reaction glaucophane + paragonite = albite + chlorite.

d) a blueschist-facies qtz-calcschist that contains aggregates of epidote + paragonite + quartz + phengite (Si_{max} = 3.28 -3.56 p.f.u.), interpreted as pseudomorphs after earlier lawsonite (CP3, filled circle). Since we have no evidence of jadeite relics formerly stable with lawsonite, we infer that breakdown of lawsonite occurred through the reaction lawsonite + albite = paragonite + zoisite + quartz at minimum pressures of 13 -14 Kbar (as suggested by Si content in phengites). The stability of Na-amphibole and garnet points to subsequent equilibration on the high-T side of the reaction paragonite + chlorite = glaucophane + garnet, in the garnet-blueschist field. Retrogression to the greenschist facies field is indicated by late-stage growth of chlorite and albite.

To sum up, the analyzed tectonic blocks of the mélange folllowed three distinct PT paths (Fig. 7c):

➢ prograde path, from lawsonite-blueschist to garnet-blueschist, followed by retrogression to epidote-blueschist facies and finally greenschist facies (solid line);

➢ eclogite facies peak, followed by blueschist- and greenschist facies retrogression (dashed line);

➢ garnet-blueschist facies peak, followed by epidote-blueschist- and greenschist facies re-equilibration (dotted line).

The different PT evolutions are not an artefact induced by different bulk compositions, because samples with similar major element (SiO_2, Al_2O_3, CaO, MgO, FeO, Na_2O) compositions exhibit substantially different PT paths.

The PT paths shown in Fig. 7c appear to converge during exhumation in the epidote-blueschist facies; the mélange matrix, in turn, records an almost complete re-equilibration in the greenschist facies, but some rare relics of Na-amphibole are still present. Therefore we can conclude that the mélange zone probably formed at least at PT conditions typical of the epidote-blueschist facies.

6. Discussion and conclusions

Three main processes can be proposed to explain the origin of the studied mélange zone:

A) metamorphism of a mélange formed during the early evolution of the subduction-accretion zone either by sedimentary processes (e.g. chaotic sedimentation, slumpings), or by tectonic processes (e.g. forearc incorporation of mafic blocks in a sedimentary matrix as a consequence of tectonic erosion);

B) tectonic mixing along a shear zone of blocks from different lithologic units; this process might have occurred during continental collision, after that tectonic coupling between the units was already accomplished in the early stages of exhumation;

C) mixing between hydrated mantle and fragments of subducted oceanic crust during rapid exhumation, as outlined by recent numerical models [3] and as proposed for the Tectonic Accretion Channels (TAC) in the Alps [29, 31].

Field and petrologic evidence enables a choice between these hypotheses. In particular:

➢ The boulders are made up of exotic lithologies, unknown in the surrounding rock units of the Voltri Massif. Notably, the mafic blocks preserving lawsonite relics, as well as the HP-metasediments with garnet, glaucophane ± Na-pyroxene have virtually no analogues in the rest of the massif. This supports the hypothesis that large-scale transport was operative during the mélange development.

➢ The various mafic and metasedimentary lithologies record a variety of peak PT conditions, ranging from blueschist- to eclogite-facies. The peak assemblages are overprinted by retrograde mineral compatibilities converging towards PT conditions typical of the epidote-blueschist facies.

➢ The mafic blocks are characterized by internal schistosities produced during HP deformation events (ranging from eclogite- to blueschist facies) unrelated to the matrix schistosity, whereas the metasedimentary blocks partially shared the same deformation history of the mélange matrix. The oldest deformation event recognizable in the matrix and in the metasedimentary blocks occurred in the blueschist-facies field, presumably during exhumation and nappe emplacement.

In the case of process (A), the whole mélange should have been subducted (and metamorphosed) as a coherent body; this implies that all the blocks should display the same metamorphic history. On the contrary, the blocks are characterized by diverse metamorphic and deformation histories; no apparent link exists between the HP-evolution of the blocks and that of the surrounding matrix before epidote-blueschist facies. As a consequence, we would exclude any mechanism involving mélange formation before subduction.

If the mélange formation is related to late-stage collisional tectonics (process B), then large-scale tectonic transport should not have occurred, and the block lithologies should have analogous in the country rocks of the mélange. Notably, the only other example of tectonic mélange reported so far in the Voltri Massif [13] occurs at the boundary between meta-ophiolitic and metasedimentary units and contains blocks deriving from both, but not exotic lithologies. As a consequence, the authors interpreted it as formed during the greenschist-facies tectonic coupling of the two units (i.e. during collision).

Therefore, the Cascine Parasi mélange zone probably originated during exhumation of deeply subducted blocks, which were tectonically incorporated in the surrounding matrix (mechanism C): strain concentration in the serpentine- and then chlorite-rich layers supplied a ductile matrix that incorporated competent blocks belonging to different tectonic levels, many of which are not currently cropping out in the rest of the massif. Ongoing deformation and displacement along the shear zone achieved exhumation and emplacement of the HP rocks to shallower levels (Fig. 8).

This mélange also shares some features with the TAC of Engi *et al*. [29]; in particular:

• they both contain eclogite and other HP-lenses of variable size confined to the mélange zone;

• they both contain fragments of variable petrographic composition, with the exception of gneissic rocks, abundant in the TAC and absent in our mélange zone;

• they both contain blocks (units) with different PT paths, indicating great mobility of the fragments prior to incorporation in the mélange;

• they are both characterized by high-strain patterns.

Mixing zones at the interface between the overriding and the subducting plate, formed during forced return flow in the subduction channel, have been predicted by numerical models [2, 3, 30]. Results of these models show similarities with occurrences in the Central Alps and in the Cyclades [31]. Other examples of tectonic mélanges containing blocks recording heterogeneous metamorphic conditions have been reported in the Maksutov complex (south Urals) [32] and in the Franciscan complex (California) [33, 32, 34]. In California the exotic blocks appear to be older than the matrix and therefore they have been interpreted as lithologies recycled in a second subduction zone after "first cycle"-HP metamorphism and exhumation [32]. Tectonic blocks of various protoliths (volcanoclastic, pelitic, gabbroic and peridotitic rocks) and different metamorphic histories are enclosed in a metasedimentary matrix in the Sanbagawa belt of Japan. Deformation responsible for this tectonic setting has been related by Takasu *et al*. [35] to exhumation processes. In the Syros island (Cyclades, Greece) a serpentinite-talc matrix mélange hosts blocks of eclogites, glaucophanites, metagabbros, impure quartzites and ultramafic rocks. Different interpretations have been suggested to explain it, the two principal being a tectonic mélange [36] and a meta-olistostrome or meta-debris flow [37, 38]. In the M. Viso area a serpentinite mélange enclosing eclogites with different temperatures of equilibration has been interpreted [39, 40] as formed in the mantle wedge during exhumation.

In conclusion, the process (C), i.e. mixing of rocks coming from different tectonic levels in a tectonic accretion channel, explains reasonably well the characteristics of our mélange

zone. We therefore suggest that the CPM was formed during forced return flow of the deeply subducted fragments inside a serpentinite-rick matrix (Fig. 8) in a subduction channel.

7. Acknowledgements

The Authors want to thank the late L. Cortesogno for sharing with them his knowledge of the outcrops, T. Gerya and B. Lombardo for fruitful discussion and useful comments. Helpful and constructive reviews by two anonymous referees are greatly appreciated. This work has been supported by MIUR COFIN project.

8. Appendix

The classification of amphiboles is after Leake *et al.* [41]. Fe^{3+} estimates have been made through charge balance approach, on the basis of 23 oxygens, assuming either a total of 13 or 15 cations (see discussion in Droop [42]).

Sample description

C 24: Omphacite grows along the rims and the cleavage planes of coarse-grained magmatic augite; a more Jd-rich omphacite grows outside the augite relics (Fig.5a). Magmatic plagioclase is replaced by aggregates of coarse-grained lawsonite (Fig.5b), omphacite, tremolite and rare jadeite. During a pervasive deformation event, the Na-clinopyroxene and lawsonite are transformed into porphyroclasts showing brittle behaviour and a pervasive schistosity develops. The Na-clinopyroxene is partially substituted by rare Na-amphibole, whereas fine-grained synkinematic lawsonite grows along the schistosity. In the pressure shadows of the Na-clinopyroxene porphyroclasts late chlorite + albite + biotite grow together with Ca-amphibole.

C 30: The oldest recognizable assemblage is Na-clinopyroxene 1 + sphene + lawsonite(?). Na-clinopyroxene 1 is an aegirinaugite with a core-to-rim increase in jadeite and, to a lesser extent, in aegirine (Fig. 5c). This assemblage is followed by the synkinematic blastesis of Na-clinopyroxene 2 + clinozoisite 1 + sphene + phengite ± paragonite: Na-clinopyroxene 2 is zoned from aegirine-rich to jadeite-rich compositions (Fig. 5c). Epidote crystals associated with Na-clinopyroxene 2 are euhedral and prismatic and could be interpreted as pseudomorphs after lawsonite. This sample therefore shows the coexistence of Na-clinopyroxene + clinozoisite, possibly preceded by the association of Na-clinopyroxene and lawsonite. Finally, a low-pressure assemblage of clinozoisite 2 + albite + chlorite develops, especially in chlorite - albite veins.

C1: metagabbro with coarse-grained relics of a Na-clinopyroxene 1 of aegirinaugitic composition, partially replaced by rare glaucophane. The stable syn-tectonic association is Na-clinopyroxene 2 + sphene + chlorite. Sphene overgrows rutile. Na-clinopyroxene 2 shows high compositional variability from aegirinaugite to omphacite; in the former plagioclase site Na-clinopyroxene 2 is closely associated with epidote. Minor retrogression results in the growth of Ca-amphibole, albite, calcite, muscovite and chlorite.

CP8: coarse-grained undeformed metagabbro with mm-sized magmatic pyroxenes replaced topotactically by a mosaic of grains of aegirinaugitic or omphacitic com-

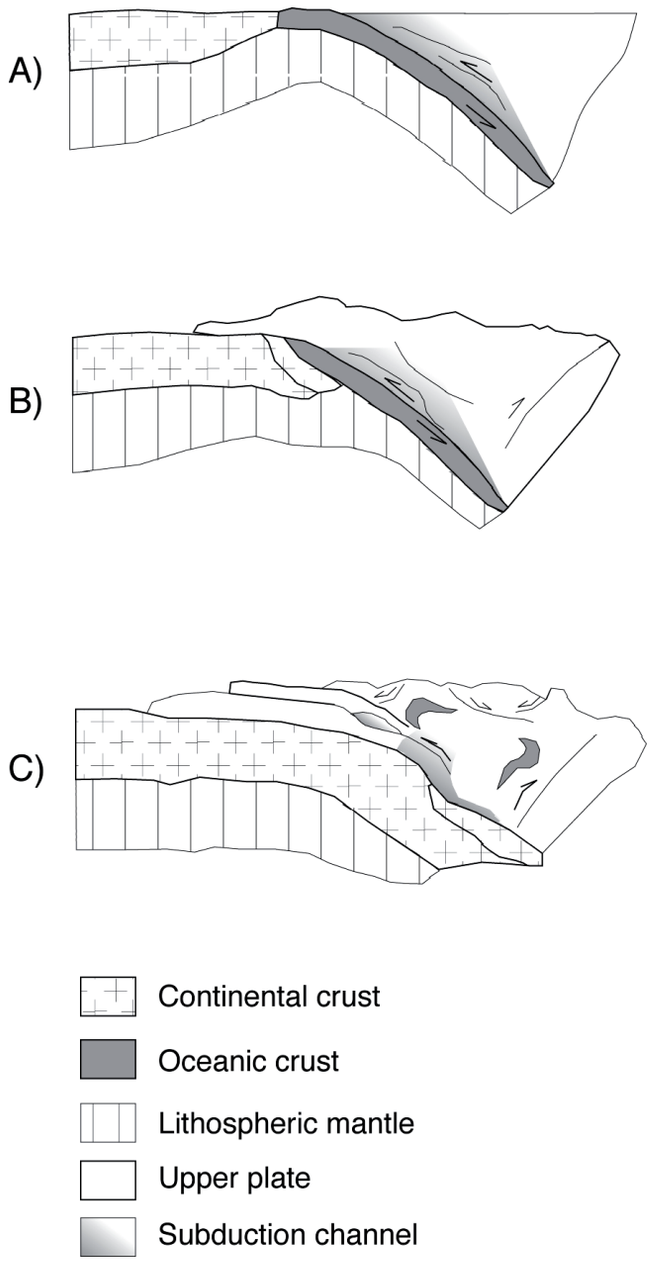

Fig. 8: cartoon which illustrates the tectonic evolution from subduction to exhumation in the Voltri Massif. **A)** subduction: a subduction channel develops at the interface between lower and upper plates [2]; **B)** exhumation and nappe emplacement: with ongoing subduction, a return flow inside the channel enables exhumation of HP rocks inside a serpentinitic mélange; **C)** collision: slowing of subduction and incipient continental collision induce further deformation in the mélange at greenschist-facies conditions.

position. These Na-clinopyroxenes are fragmented and a new generation of omphacitic pyroxene grows from the fragments. In the plagioclase site epidote and phengite are closely intergrown. Epidote is zoned, usually with Fe content decreasing from core to rim.

C27: eclogitic metabasite showing rare coarse-grained relics of Na-clinopyroxene 1 replacing older Na-amphibole. Garnet is characterized by a prograde core-to-rim zonation from $Alm_{(24-38)}Prp_{(0,2-1,5)}Grs_{(25-27)}Sps_{(34-48)}$ to $Alm_{(64-67)}Prp_{(2-3)}Grs_{(22-23)}Sps_{(8-9)}$ and sometimes contains 10 microns-wide inclusions of Fe-glaucophane. Na-clinopyroxene 2 ranging in composition from omphacite to aegirinaugite (Fig. 5d) grows along the schistosity, together with sphene. Chlorite and phengite (Si^{4+} = 3,24-3,28 p.f.u.) show equilibrium textures with Na-clinopyroxene 2, but are poorly oriented along the fabric and are interpreted as post-tectonic. Finally a greenschist-facies assemblage of chlorite, albite, epidote and muscovite develops.

CP5: this metabasalt underwent a complex metamorphic history, beginning from eclogite equilibration, as shown by the assemblage: aegirinaugite + almandine-rich garnet + Na - amphibole 1. The eclogite assemblage is preserved only inside microdomains bounded by the blueschist foliation with the stable assemblage of Na - amphibole 2 + phengite (Si^{4+} = 3,48-3,50 p.f.u.) + epidote + sphene. Garnet displays a prograde core-to-rim zonation from $Alm_{(45)}Prp_{(0,7-0,8)}Grs_{(24-26)}Sps_{(29-30)}$ to $Alm_{(53-62)}Prp_{(0,4-0,7)}Grs_{(20-21)}Sps_{(17)}$. Late - stage retrogression involves growth of chlorite and Na - Ca amphibole on Na - amphibole and of white mica + albite + chlorite on epidote. Some Na -clinopyroxene and Na-amphibole inclusions are found inside garnet. All Na-amphiboles fall in the Fe-glaucophane field.

CP2: blueschist metabasalt which displays a pervasive schistosity with Na-amphibole 2 + epidote + phengite (Si^{4+} = 3,46-3,58 p.f.u.) + sphene. Porphyroclasts of almandine-rich garnet ($Alm_{(54-57)}Prp_{(0,4)}Grs_{(20-21)}Sps_{(25-30)}$), Na - amphibole 1 and rutile are present. Na-amphibole composition falls in the Fe-glaucophane field. Late chlorite and albite partially replace garnet and Na - amphibole. Inclusions of Fe-glaucophane are rarely found inside garnet and inclusions of sphene and phengite inside Na-amphibole 1. This sample therefore underwent a first equilibration stage in the garnet-blueschist facies, followed by pervasive re-equilibration in the epidote-blueschist facies and late-stage minor growth of greenschist-facies minerals.

VR81: this metabasite possibly derives from recrystallization of an ophiolitic detritus, in view of the K_2O enrichment unusual for a metabasalt (up to 1,8 wt%). It is characterized by an assemblage of Na - amphibole 2 (glaucophane to Fe-glaucophane) + phengite (Si^{4+} = 3,37-3,56 p.f.u.) + Fe-epidote + sphene and by coarse -grained porphyroclasts of Na - amphibole 1, of garnet and of rutile. Na-amphibole inclusions are found inside garnet. Na - amphibole is partially replaced by Na-Ca-amphibole and garnet by chlorite.

C9: blueschist metabasalt with an assemblage of Na-amphibole 1 + almandine-rich garnet ($Alm_{(51-63)}Prp_{(0,4-0,8)}Grs_{(22-25)}Sps_{(13-23)}$) + phengite 1 + sphene, followed by the blastesis of synkinematic finer-grained Na-amphibole 2 + phengite 2 (Si^{4+} = 3,45-3,46 p.f.u.) + epidote + sphene. Na-amphiboles show compositions ranging from Fe-glaucophane to glaucophane. Inclusions of sphene and, more rarely, of phengite are present inside Na-amphibole 1. Aggregates of phengite + chlorite + biotite ± paragonite (Fig. 5e) can be interpreted as pseudomorphs after lawsonite (e.g. Ballèvre *et al*. [43]); they contain inclusion trails of sphene (Fig. 5e). Rare crystals of Na-amphibole are present near the rims and in the strain shadows around the pseudomorphs. The breakdown products in the pseudomorphs are not oriented. Garnet relics are partially replaced by chlorite + calcite + quartz ± albite. This sample therefore shows a transition from lawsonite-blueschist to garnet-blueschist and finally to epidote-blueschist facies equilibration.

C8: this sample is a quartzschist with synkinematic peak assemblage in the garnet-blueschist facies: Na-amphibole + garnet + phengite (Si^{4+} = 3,32-3,38 p.f.u.) + epidote + quartz ± sphene ± apatite ± ores (Fig. 5f). Na-amphibole is glaucophane and shows a core to rim increase in Fe^{2+} and decrease in Mg. Garnet is Mn-rich and occurs both as small inclusions inside Na-amphibole and epidote and as fine-grained post-kinematic crystals. The matrix grains display a core-to rim zonation from $Alm_{(11-12)}Prp_{(2-3)}Grs_{(11)}Sps_{(75)}$ to $Alm_{(30-32)}Prp_{(2-3)}Grs_{(6-7)}Sps_{(58-63)}$. The inclusions share the same composition of the cores of the matrix grains. Epidote usually has REE-rich cores. Late-stage growth of Ca-amphibole and albite (± chlorite ± calcite) points to a local greenschist-facies retrogression.

C 13: quartzschist characterized by a stable blueschist-facies synkinematic assemblage of Na-amphibole + phengite (Si^{4+} = 3,50 - 3,77 p.f.u.) + epidote + quartz. Coarse-grained Na-amphiboles show pronounced core-to-rim decrease in Mg and increase in Fe content and pass from glaucophane cores to Mg-riebeckite rims. The finer-grained amphibole crystals usually do not display the more external, Mg-riebeckitic rim. Rare porphyroclasts of Na-clinopyroxene have aegirine cores and rims of aegirinaugite composition. Some Mn-rich garnets ($Alm_{(11-20)}Prp_{(0,7-2)}Grs_{(7-11)}Sps_{(71-77)}$) are included in both Na-amphibole and Na-pyroxene. Finally, a retrogressive event produced growth of calcite and of biotite on phengite.

CP3: blueschist-facies qtz-calcschist with alternating bands rich in Na - amphibole 2 (Fe-glaucophane) + phengite (Si^{4+} = 3,48-3,57 p.f.u.) + chlorite + epidote and bands rich in quartz and carbonates. Porphyroclasts of Na - amphibole 1 and aggregates of epidote + paragonite + quartz + phengite (Si^{4+} = 3,28-3,56 p.f.u.) are present (Fig. 5g). They likely represent pseudomorphs after earlier lawsonite, probably formed during a prograde stage (see par. 5). Epidote shows sometimes cores rich in allanite. Some Mn-rich garnets ($Alm_{(27-40)}Prp_{(0,4-2)}Grs_{(15-19)}Sps_{(40-54)}$) with typical skeletal texture are present in the quartz-rich layers. Late-stage chlorite and albite partially overgrow Na -amphibole and garnet.

C46: quartzschist with a well defined metamorphic layering, defined by Na-amphibole- and Na-clinopyroxene-rich layers. This layering issues from a folding event with isoclinal folds (Fig.5h) and possibly reflects an original compositional

banding. The synkinematic assemblage is: glaucophane + garnet + phengite + quartz + apatite in the Na-amphibole-rich layers, and aegirinaugite + garnet + phengite + quartz ± glaucophane in the Na-clinopyroxene-rich layers. Some coarse-grained garnets show a core-to-rim zonation from $Alm_{(17-18)}Prp_{(0,7-0,9)}Grs_{(19-24)}Sps_{(58-62)}$ to $Alm_{(37-48)}Prp_{(2-2,5)}Grs_{(20)}Sps_{(30-41)}$; fine-grained garnets display compositions either similar to the cores or to the rims of the coarser grains. The cores of the bigger garnets are crowded with inclusions of magnetite, Mg-amphiboles and rutile. Phengites are characterized by Si^{4+} content of 3,65-3,78 p.f.u. Na-clinopyroxene is later partially overgrown by Na-Ca amphiboles and phengite by biotite.

9. References

[1] Raymond L.A., Classification of melanges, in: Raymond L.A. (ed.), Melanges: their nature, origin, and significance, Geological Society of America Special Paper 198, 1984, pp. 7–20.

[2] Gerya T.V., Stöckhert B., Perchuk A.L., Exhumation of high-pressure metamorphic rocks in a subduction channel: a numerical simulation. Tectonics, 21(6) (2002) 1056, doi: 1029/2002TC001406.

[3] Stöckhert B., Gerya T.V., Pre-collisional high pressure metamorphism and nappe tectonics at active continental margins: a numerical simulation. Terra Nova 17 (2) (2005) 102-110.

[4] Messiga B., Scambelluri M., Retrograde PT-t path for the Voltri Massif eclogites (Ligurian Alps, Italy): some tectonic implications. J. Metamorphic Geol. 9 (1991) 93-109.

[5] Messiga B., Scambelluri M., Piccardo G.B., Chloritoid-bearing assemblages in mafic systems and the eclogite-facies hydration of alpine Mg-Al metagabbros (Erro-Tobbio unit, Ligurian Western Alps). European Journal of Mineralogy 7 (1995) 1149-1167.

[6] Liou J.G., Zhang R., Ernst W.G., Liu J., McLimans R., Mineral parageneses in the Piampaludo eclogitic body, Gruppo di Voltri, Western Ligurian Alps. Schweiz. Mineral. Petrogr. Mitt. 78 (1998) 317-335.

[7] Cimmino F., Messiga B., I calcescisti del Gruppo di Voltri (Liguria Occidentale): le variazioni composizionali delle miche bianche in rapporto alla evoluzione tettonico-metamorfica alpina. Ofioliti 4 (3) (1979) 269-294.

[8] Messiga B., Alpine metamorphic evolution of Ligurian Alps (North-West Italy): chemography and petrological constraints inferred from metamorphic climax assemblages. Contributions to Mineralogy and Petrology 95 (1987) 269-277.

[9] Capponi G., Crispini L., Structural and metamorphic signature of Alpine tectonics in the Voltri Massif (Ligurian Alps, North-Western Italy). Eclogae geol. Helv. 95 (2002) 31 - 42.

[10] Crispini L., Frezzotti M.L., Fluid inclusion evidence for progressive folding in metasediments of the Voltri Group (Western Alps, Italy). Journal of Structural Geology 20 (12) (1998) 1733-1746.

[11] Capponi G., Crispini L., Progressive shear deformation in the metasediments of the Voltri Group (Ligurian Alps, Italy): occurrence of structures recording extension parallel to the regional foliation. Boll. Soc. Geol. It. 116 (1997) 267 - 277.

[12] Wheeler J., Butler R.W.H., Criteria for identifying structures related to true extension in orogens. Journal of Structural Geology 16 (1994) 1023-1027.

[13] Vissers R. L. M., Hoogerduijn Strating E.H., Heimans M. & Krabbendam M., Structures and microstructures in a thrust related, greenschist-facies tectonic mélange, Voltri Group (NW Italy). Ofioliti 26 (1) (2001) 33-46.

[14] Vanossi M., Cortesogno L., Galbiati B., Messiga B., Piccardo G. & Vannucci R., Geologia delle Alpi Liguri: dati, problemi, ipotesi. Memorie della Società Geologica Italiana 28 (1984) 5-75.

[15] Polino R., Dal Piaz G.V., Gosso G. Tectonic erosion at the Adria margin and accretionary processes for the Cretaceous orogeny of the Alps. Vol. spec. Soc. Geol. Italiana n°1 (1990) 345-367.

[16] Kretz R., Symbols for rock-forming minerals. Amer. Mineral. 68 (1983) 277-279.

[17] Sanford R.S., Metamorphism, diffusion and metasomatism in an ultramafic blackwall zone, Blandford, Massachusetts. Abstracts with Programs - GSA v. 10, n.2 (1978) p. 84.

[18] Purcell E., Metasomatism of black-wall reaction zones of Syros, Greece. Keck Seventeenth Research Symposium in Geology, Greece, (2004) 46-49.

[19] Poli S., Schmidt M.W., H2O transport and release in subduction zones: Experimental constraints on basaltic and andesitic systems. Journal of Geophysical Research, 100 (B11) (1995) 22.299-22.314.

[20] Maruyama S., Moonsup C., Liou J.G., Experimental investigations of blueschist-grenschist transition equilibria: pressure dependence of Al_2O_3 contents in sodic amphiboles - a new geobarometer. Geological Society of America Memoir 164 (1986) 1-16.

[21] Connolly J. A. D. Calculation of multivariable phase diagrams: an algorithm based on generalized thermodynamics. American Journal of Science 290 (1990) 666-718.

[22] Koons P.O., An experimental investigation of the behavior of amphibole in the system Na_2O - MgO - Al_2O_3 - SiO_2 - H_2O at high pressures. Contributions to Mineralogy and Petrology 79 (1982) 258-267.

[23] Guillot S., de Sigoyer J., Lardeaux J.M., Mascle G., Eclogitic metasediments from the Tso Morari area (Ladakh, Himalaya): evidence for continental subduction during India-Asia convergence. Contributions to Mineralogy and Petrology 128 (1997) 197-212.

[24] Massonne H-J., Schreyer W., Phengite geobarometry based on the limiting assemblage with K-feldspar, phlogopite, and quartz. Contributions to Mineralogy and Petrology 96 (1987) 212-224.

[25] Maresch W.V., Experimental study on glaucophane: an analysis on present knowledge. Tectonophysics 43 (1977) 109-125.

[26] Guiraud M., Holland T., Powell R., Calculated mineral equilibria in the greenschist-blueschist-eclogite facies in NaO_2 - FeO - MgO-Al_2O_3 - SiO_2 - H_2O: methods, results and geological applications, Contributions to Mineralogy and Petrolgy 104 (1990) 85-98.

[27] Proyer A., Metamorphism of pelites in NKFMASH - a new petrogenetic grid with implications for the preservation of high-pressure mineral assemblage during exhumation. J. metamorphic Geol., 21 (2003) 493-509.

[28] Green T.H. and Hellman P.L., Fe-Mg partitioning between coexisting garnet and phengite at high pressure, and comments on a garnet-phengite geothermometer. Lithos 15 (1982) 253-266.

[29] Engi M., Berger A., Roselle G.T., Role of tectonic accretion channel in collisional orogeny. Geology, 29(12) (2001) 1143-1146.

[30] Schwartz S., Allemand P., Guillot S., Numerical model of the effect of serpentinites on the exhumation of eclogitic rocks: insights from the Monviso ophiolitic massif (Western Alps). Tectonophysics 342 (2001) 193-206.

[31] Engi M., Berger A., Rohrbach L., Anatomy of mélange zones in tectonic accretion channels: relation to the mixing zones predicted by numerical models. Geophysical Research Abstracts, vol. 7 (2005) 09386.

[32] Dobretsov N.L., Blueschists and eclogites: a possible plate tectonic mechanism for their emplacement from the upper mantle. Tectonophysics 186 (1991) 253-268.

[33] Cloos M., Flow melanges: Numerical modeling and geologic constraints on their origin in the Franciscan subduction complex, California. Geological Society of America Bulletin 93 (1982) 330-345.

[34] Anczkiewicz R., Platt J.P., Thirlwall M.T., Wakabayashi J., Franciscan subduction off to a slow start: evidence from high-precision Lu-Hf garnet ages on high grade-blocks. Earth and Planetary Science Letters 225 (2004) 147-161.

[35] Takasu A., Wallis S.R., Banno S., Dallmeyer R.D., Evolution of the Sanbagawa metamorphic belt, Japan. Lithos 33 (1994)119-133.

[36] Altherr R., Seidel E., Speculations on the geodynamic evolution of the Attic-Cycladic crystalline complex during alpidic times. Proceedings of the VI Colloquium on the Geology of the Aegean Region, Athens, 1 (1977) 347-52.

[37] Dixon J.E., Ridley J.R., Syros, in Helgeson H.C. (Ed.), Chemical transport in metasomatic processes, Dordrecht, Reidel, 1987, pp. 489-501.

[38] Brocker M., Enders M., U-Pb geochronology of unusual eclogite-facies rocks from Syros and Tinos (Cyclades, Greece). Geol. Mag. 136 (2) (1999) 111-118.

[39] Blake M.C., Moore D.E., Jayko A.S. The role of serpentinite melanges in the unroofing of UHPM rocks: an example from the Western Alps of Italy, in: Coleman R.G., Wang X. (Eds.), Ultrahigh pressure metamorphism, Cambridge University Press, 1995, pp.182-205.

[40] Schwartz S., Lardeax J.-M., Guillot S., Tricart P., Diversité du métamorphisme éclogitique dans le massif ophiolitique du Monviso (Alpes occidentales, Italie). Geodinamica Acta 13 (2000) 169-188.

[41] Leake B.E. et al., Nomenclature of amphiboles: Report of the Subcommittee on Amphiboles of the International Mineralogical Association, Commission on New Minerals and Mineral Names. American Mineralogist 82 (9–10) (1997) 1019–1037.

[42] Droop G.T.R., A general equation for estimating Fe3+ concentrations in ferromagnesian silicates and oxides from microprobe analyses, using stoichiometric criteria. Mineralogical Magazine (51) 431-435.

[43] Ballèvre M., Pitra P., Bohn M. Lawsonite growth in the epidote blueschists from the Ile de Groix (Armorican Massif, France): a potential geobarometer. Journal of metamorphic Geology, 21 (2003) 723-735.